

Determination of conformational energy differences of propynlidyne isomers using the effective valence shell Hamiltonian method

Rajat K. Chaudhuri^{a)} and Sonjoy Majumder
Indian Institute of Astrophysics, Bangalore-560034, India

Karl F. Freed^{b)}
The James Franck Institute and the Department of Chemistry, The University of Chicago, Chicago, Illinois 60637

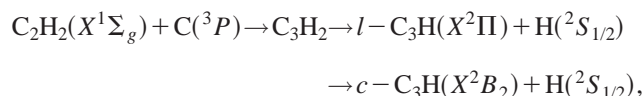
(Received 30 March 1999; accepted 9 March 2000)

We have applied the highly correlated *ab initio* effective valence shell Hamiltonian (H^v) method to determine the energy difference between the cyclic and linear isomers of propynlidyne (C_3H). Calculations are also described for the vertical excitation energies, ionization potentials, electron affinities, dipole moments, oscillator strengths, and some harmonic vibrational frequencies, which are all determined using the third order H^v method. Computations at both the experimental and theoretically optimized geometries are used to illustrate the geometrical dependence of the computed properties. The H^v optimized geometry is obtained using a two-configurational reference function describing the two dominant resonance structures. Our third-order vertical excitation energy to the lowest excited state in the cyclic isomer, dipole moments, and ground state isomer conformational energy difference are all in good agreement with experiment and with other highly correlated many-body calculations. The computations for higher excited states and for ionization potentials, electron affinities, and oscillator strengths represent the first reports of these quantities. An explanation is provided for persistent theoretical difficulties in computing b_1 bending vibrational frequencies of the cyclic isomer. © 2000 American Institute of Physics.
 [S0021-9606(00)30321-X]

I. INTRODUCTION

The understanding of hydrocarbon syntheses in interstellar clouds provides one stimulus for increased recent interest in studying the hydrocarbon radical C_3H and its isomers. The linear C_3H radical (propynlidyne) has first been detected in TMC-1 and the carbon star IRC+ 10216 by Thaddeus *et al.*¹ using microwave spectroscopy and by Gottlieb *et al.*² in the laboratory. Two years later Yamamoto *et al.*³ discovered the cyclic isomer (cyclo-propynlidyne) c - C_3H in TMC-1. Standard reaction models, based on radiative association, dissociative recombination, and exothermic ion-molecule processes,^{4,5} fail to reproduce the observed number densities and isomer ratios for the linear and cyclic C_3H isomers. Therefore, explaining the formation of C_3H from its precursors remains an active area of research.

The computation of this isomer energy difference has been a major theoretical challenge. The earliest UHF/6-31G** *ab initio* calculations for C_3H by Yamamoto *et al.*³ provided the belief that cyclic C_3H is less stable than the linear C_3H isomer. However, this initial belief has been reversed by subsequent state-of-the-art theoretical calculations and experiments. Kaiser *et al.*^{6,7} use coupled cluster calculations with single, double, and partial triple excitations [CCSD(T)] to supplement their experimental investigation of the mechanism for the atom-neutral reaction,



in a study of the dynamical processes involved in the formation of various C_3H isomers. Multireference configuration interaction (MRCI) calculations by Takahashi *et al.*⁸ support the conclusions by Kaiser *et al.*⁶ that the c - C_3H (cyclic C_3H) radical is energetically more stable than the l - C_3H (linear C_3H) isomer. While the computed ground state energy difference between these two isomers from the MRCI and CCSD(T) methods are quite close to experiment, the same quantity generated from other theoretical approaches departs widely^{3,9} from experiment. These large discrepancies emerge primarily from methodological differences among the various approaches and, perhaps, from basis set deficiencies. In addition, although considerable progress has been made in understanding the dynamics of the bond rupture reaction of the C_3H_2 radical and the geometries and the relative energies of the C_3H isomers, only a few studies^{8,10} have so far attempted to describe the properties of the lowest excited state of the C_3H isomers and their ionization potentials and electron affinities.

The present work describes theoretical calculations for the ground and excited state properties of both C_3H isomers. Almost all previous theoretical works concur that a bent geometry (C_s point group) is energetically higher than the linear isomer [see Refs. 7 and 11 for details] and that the cyclic isomer is more stable than the linear C_3H isomer. Since the earlier MP2/6-31G(d, p) optimization⁸ produces a rather

^{a)}Present address: The James Franck Institute and the Department of Chemistry, The University of Chicago, Chicago, IL 60637.

^{b)}Electronic mail: freed@kffl.uchicago.edu

poor geometry, presumably partially because of the presence of two relevant resonance structures, we consider the geometry optimization using the H^v method with a two-configuration reference space that contains these relevant resonance structures. The ground and excited state properties of the l - and c - C_3H radicals are computed through third order with the H^v method for both H^v optimized geometries, as well as for the experimental and MP2/6-31G(d, p) optimized geometries for comparison. Several harmonic vibrational frequencies are obtained as a by-product of the optimization procedure. Extensive theoretical studies¹²⁻²⁴ document the H^v formalism, its conceptual advantages, the computational algorithms for evaluating atomic and molecular properties, and the higher-order convergence behavior of the method.²⁵

The computation of the conformational energy difference is complicated within a number of methods by symmetry breaking in the treatment of the linear isomer. The ground state of the l - C_3H isomer is of ${}^2\Pi$ symmetry, with one electron occupying the outer most degenerate π orbital. Maintaining this degeneracy during the optimization procedure often imposes significant technical problems. We impose the degeneracy of the l - C_3H isomer by using orbitals taken from a series of self-consistent field (SCF) calculations for the positive ion and the neutral species. More specifically, all doubly occupied orbitals for the ground state are determined from a closed shell SCF calculation for the ground state of the positive ion. The singly occupied π orbital and the other valence shell orbitals are generated as improved virtual orbitals (IVOs) for the neutral species.¹² Although symmetry breaking problems do not arise for the cyclic isomer, a similar procedure has also been applied for this case in order to treat both the isomers on an equal footing. Moreover, computations using this mixed orbital scheme for the cyclic isomer are in excellent agreement with those produced with our standard approach based on using neutral molecule ground SCF orbitals for all the occupied orbitals, an agreement similar to that demonstrated in many previous examples as emerging from the relative insensitivity of third order effective valence shell Hamiltonian calculations to a wide range of different orbital choices.²⁶

In Sec. II we present a brief overview of the H^v method for calculating energies and other molecular properties, such as dipole and transition dipole moments. The computed results are presented and discussed in Secs. III and IV, respectively. We provide the first high level *ab initio* computations for excited electronic states above the lowest, the oscillator strengths for these transitions, and the ionization potentials and electron affinities. An explanation is given for persistent theoretical difficulties in computing reasonable frequencies for the b_1 bending vibrations of the cyclic isomer.

II. THEORY

Perturbation theory proceeds by decomposing the molecular electronic Hamiltonian H into a zeroth-order part H_0 and a perturbation V ,

$$H = H_0 + V, \quad (2.1)$$

where H_0 is constructed here as a sum of one-electron Fock operators. The full many-electron Hilbert space is then par-

tioned into a primary space (also called model or reference space) with projector P and its orthogonal complement with projector $Q = 1 - P$. The P space spans the valence space of all distinct configuration state functions involving a filled core and remaining electrons distributed among the valence orbitals in all possible ways to ensure completeness of the P -space. Hence, the Q -space contains all basis functions with at least one core-hole and/or one occupied-excited orbital. The H^v method transforms the full Schrödinger equation,

$$H\Psi_i = E\Psi_i, \quad (2.2)$$

into the P -space effective valence-shell Schrödinger equation,

$$H^v\Psi_i^v = E\Psi_i^v, \quad (2.3)$$

where the valence space projections $\Psi_i^v = P\Psi_i$ are the projections of the exact eigenfunctions and the energies E are the corresponding exact eigenvalues of the full Schrödinger equation. The H^v method provides the unique Hermitian approximation, which through second order is

$$H^v = PHP + \frac{1}{2} \sum_{\Lambda, \Lambda'} [P(\Lambda)VQ(E_\Lambda - H_0)^{-1}QVP(\Lambda') + \text{h.c.}], \quad (2.4)$$

where h.c. designates the Hermitian conjugate of the preceding term and $P(\Lambda)$ designates the projector onto the valence space basis function $|\Lambda\rangle$.

In order to compute the diagonal and off-diagonal matrix elements of an operator A between the normalized full space wave functions Ψ_i within H^v theory, the matrix elements $\langle\Psi_i|A|\Psi_i'\rangle$ are transformed into the matrix elements of an effective valence shell operator A^v between the orthonormal valence space H^v eigenfunctions Ψ_i^v , i.e.,

$$\langle\Psi_i|A|\Psi_i'\rangle = \langle\Psi_i^v|A^v|\Psi_i'^v\rangle. \quad (2.5)$$

The effective operator A^v can likewise be expanded perturbatively, and through leading order in the perturbative corrections A^v is evaluated as

$$A^v = PAP + \frac{1}{2} \sum_{\Lambda, \Lambda'} [P(\Lambda)VQ(E_\Lambda - H_0)^{-1}QAP(\Lambda') + \text{h.c.}]. \quad (2.6)$$

Thus, the expectation values and off-diagonal couplings may be determined by first solving Eqs. (2.3) and (2.6) and then by taking the corresponding matrix elements on the right-hand side of Eq. (2.5). Once A^v is evaluated, it furnishes all diagonal and off-diagonal matrix elements within the P -space states. Many-body theory techniques can be applied to reduce Eq. (2.6) and thereby express the matrix elements of A^v directly in the valence orbital basis. The resulting equations are available elsewhere¹³ in terms of core-, one-, two-,... electron valence shell operators $A_c^v, A_i^v, A_{ij}^v, \dots$, respectively, in the operator representation,

$$A^v = A_c^v + \sum_i A_i^v + \frac{1}{2} \sum_{i,j} A_{ij}^v + \dots, \quad (2.7)$$

TABLE I. Structural data for the C₃H isomers.

Parameter	Linear				Cyclic			
	MP2 geometry ^a (Å)	Experimental ^b (Å)	H ^v geometry (Å)	CCSD(T) ^c (Å)	MP2 geometry ^a (Å)	Experimental ^d (Å)	H ^v geometry (Å)	CCSD(T) ^c (Å)
R(C1–H)	1.0631	1.0171	1.07	1.065	1.0790	1.0760	1.079	1.078
R(C1–C2)	1.2005	1.2539	1.255	1.243	1.3747	1.3739	1.3709	1.377
R(C2–C3)	1.3640	1.3263	1.340	1.347	1.3878	1.3771	1.3763	1.378

^aReference 8.^bReference 27.^cReference 6.^dReference 11.

where A_c^v is the constant core contribution and A_i^v is a one-electron effective operator with matrix elements $\langle v|A_i^v|v' \rangle$ in the valence orbital basis $\{v\}$. The effective dipole operator A^v acts only on functions in P -space, i.e., the valence space. Although the dipole operator is a one-electron operator, two-electron effective operators A_{ij}^v appear in the lowest-order nontrivial correction from the perturbation expansion in Eq. (2.6). The nonclassical two-electron terms are necessary to provide accurate dipole and transition moments. In our computations, the effective Hamiltonian H^v is first diagonalized to obtain its eigenvalues and eigenfunctions Ψ_i^v . The latter are then employed along with Eq. (2.5) to compute expectation values and transition moments of the operator A by use of the effective valence shell operator A^v which is evaluated from Eq. (2.6).

III. COMPUTATIONAL DETAILS

All energies and molecular properties are evaluated for the c - and l -C₃H radicals at the experimental^{11,27} and theoretically optimized MP2⁸ and H^v geometries. (See Table I for details and the discussion below.) The ground states of the cyclic and linear C₃H isomers belong to the C_{2v} and $C_{\infty v}$ point groups, respectively. The restricted open-shell Hartree–Fock approximation (ROHF) to the ground state of the cyclic isomer is a single determinant with six doubly occupied a_1 orbitals, one doubly occupied b_2 orbital, and two doubly and one singly occupied b_1 orbitals. Thus, the ground state of cyclic C₃H radical is of 2B_1 symmetry. The ground state of linear C₃H, on the other hand, has ${}^2\Pi$ symmetry, with seven doubly occupied σ orbitals and two doubly and one singly occupied π orbitals.

The carbon atom basis set is constructed from a $(10s7p2d)/[5s3p2d]$ contracted Gaussian basis of Sadlej,²⁸ augmented by two s diffuse functions with exponents 0.021 and 0.0055, two p diffuse functions with exponents 0.021 and 0.0049, and one d diffuse function with exponent 0.015 for each of the carbon atoms. The hydrogen atom basis is a $(5s2p)/[3s2p]$ basis.²⁹ This provides a basis of 120 contracted Gaussian type orbitals (CGTOs). The number of CGTOs used in this basis is quite close to that (a TZPP basis) employed by Ochsenfeld *et al.*³⁰ The geometries of both isomers have been optimized by computing the third-order H^v energy using a two-orbital reference space. The MP2 optimized geometries (see Table I) are quite similar to the experimental geometry for the c -C₃H radical with the

maximum deviation in bond lengths of 0.01 Å. In contrast, calculations for the linear isomer yield a much larger discrepancy between the MP2, on the one hand, and the H^v and experimental geometries on the other hand. The poor quality of the MP2 geometry for the linear isomer arises because a one-configuration reference function is inadequate to describe the competition between the two dominant C–C≡C–H and C=C=C–H resonance structures. The MP2 geometry weighs the latter structure too heavily, while the H^v geometry optimization uses a minimal double reference treatment (see below) that adequately describes the mixing between these two resonance structures. All computations (optimization) produce a longer C–H bond length than experimental²⁷ which actually only determines the projection of the C–H bond on the molecular axis. We, however, find no evidence for a bent C–H bond, although all atomic displacements have not been considered.

A four-orbital H^v valence space (a complete active space) is used for computing the state energies and properties of both isomers at the experimental and optimized geometries. The choice of valence space orbitals is primarily based on energy considerations and the contributions of various orbitals to the states of interest¹⁸ as illustrated below. The valence space generally spans a number of the highest occupied molecular orbitals in the ground state SCF approximations and a number of the lowest unoccupied orbitals in this state. For the cyclic geometry, the four-orbital valence orbital space comprises two a_1 orbitals (one occupied and one unoccupied), one b_1 orbital (the singly occupied orbital in the ground state), and one b_2 (unoccupied) orbital. The complete active space for the linear geometry is composed of two σ (one occupied and one unoccupied) and two π (one singly occupied and one unoccupied) orbitals.

It is important to note the significant difference in the choice of both orbitals and orbital energies between the H^v and traditional multireference perturbation methods.^{31,32} The traditional approach generates all orbitals and their energies from a single Fock operator (the ground state Fock operator). Thus, all reference space orbitals and orbital energies, including those that are either occupied or unoccupied in the ground state SCF approximation, are evaluated using the same potential. The unoccupied reference space orbitals generated through this procedure describe an electron in the field of N others and are consequently more appropriate for describing negative ion states than the low-lying excited states

TABLE II. Vertical excitation energies (in eV) and oscillator strengths (in parentheses) of the *c*-C₃H radical.

State	Third-order H ^v			CASSCF ^a	EOMCC-IP ^b	Experiment ^c
	MP2 geometry	Experimental geometry	H ^v geometry			
1 ² A ₁	1.377 (0.037)	1.347 (0.037)	1.418 (0.039)	1.149	1.283	1.339
1 ⁴ A ₂	3.735	3.754	3.754			
1 ² B ₂	3.891	3.908	3.858			
1 ² A ₂	4.573 (0.014)	4.578 (0.014)	4.590 (0.014)			
2 ² A ₁	7.825	7.775	7.778			
2 ⁴ B ₁	8.439	8.313	8.427			
2 ² B ₁	8.572	8.445	8.559			
2 ² A ₂	8.814	8.733	8.767			

^aReference 8.^bReference 10.^cReference 26.

of interest. The H^v method, on the other hand, determines the unoccupied reference space orbitals and their energies as improved virtual orbitals (IVOs) from a set of V^{N-1} potential Fock operators in order to optimize the first-order description [from PHP in Eq. (2.4)] and thereby to minimize the higher-order perturbative corrections.^{17,18,24}

The H^v method thus yields unoccupied reference space orbital energies that are much lower than those from the ground state Fock operator due to the absence of an extra Coulomb operator in the H^v treatment for the IVOs. After the H^v valence space and orbital energies are computed in this fashion, the reference space orbital energies are replaced by their democratic average to eliminate (or greatly reduce) convergence difficulties from so-called intruder states.²⁵

The explicit procedure for obtaining the molecular orbitals and their energies involves a sequence of self-consistency field (SCF) calculations. (Some steps may actually be obtained using a single unitary transformation.²⁰) For example, the four-orbital reference space for the *c*-C₃H radical is generated by the sequence of SCF calculations

- (1) (core)¹⁶6a₁²3b₁¹, ²B₁,
- (2) [(core)¹⁶6a₁²3b₁⁰]2b₂¹, ²B₂,
- (3) [(core)¹⁶6a₁²3b₁⁰]7a₁¹, ²A₁.

Here, the first step is a X²B₁ state SCF calculation, and steps (2) and (3) are independent single orbital optimizations for the indicated states, where the orbitals inside the square brackets are frozen as the orbitals determined in the previous steps. The excited orbitals are then obtained by diagonalizing the X²B₁ state Fock operator in the orbital space comple-

mentary to the union of the core and valence spaces. The H^v method incorporates correlation contributions arising from single and double excitations out of all the core orbitals and therefore requires fewer core orbitals in the valence space than CASSCF methods that omit the core excitations. As noted in the Introduction, the retention of strict degeneracy for the linear isomer is accomplished by using a mixture of positive and neutral orbitals. When this type of scheme is applied to the cyclic isomer, step (1) of the above sequence is replaced by the two steps

- (1) (core)¹⁶6a₁², ¹A₁,
- (1') [(core)¹⁶6a₁²]3b₁¹, ²B₁,

while steps (2) and (3) remain unchanged. A comparison of computations for the cyclic isomer with both orbital choices provides a test of its accuracy.

Because of the large number of computed points required for optimizing the calculations for the H^v geometry optimization, the H^v geometries are performed with the more limited two-orbital reference space. The core and valence orbitals are determined from the SCF sequence,

- (1) (core)¹⁶7σ², ¹Σ,
- (2) [(core)¹⁶7σ²]2π¹, ²Π,
- (3) [(core)¹⁶7σ²2π⁰]2π'¹, ²Π,

for the linear isomer. This H^v geometry optimization is of interest as a nontrivial test for the H^v analytical derivative method³³ for which computer codes are currently under development.

TABLE III. Vertical ionization potentials and electron affinities (in eV) of the *c*-C₃H radical.

State	Third-order H ^v		
	MP2 geometry	Experimental geometry	H ^v geometry
Ionization potential			
1 ¹ B ₁	10.708	10.665	10.666
1 ¹ A ₁	10.711	10.674	10.706
Electron affinity			
1 ¹ A ₁	1.804	1.732	1.741
1 ¹ B ₁	-0.509	-0.494	-0.512
1 ³ B ₁	-0.522	-0.505	-0.524

TABLE IV. Dipole moments (in Debye) of the c -C₃H radicals.

State	Third-order H ^v			EOMCC-IP ^a	MP2 ^b	CASSCF ^b	Experiment
	MP2 geometry	Experimental geometry	H ^v geometry				
X ² B ₁	2.43	2.42	2.44	2.35	2.34	2.37	2.30 ^c
1 ² A ₁	4.31	4.25	4.28	3.03			
1 ⁴ A ₂	1.80	1.72	1.75				
1 ² B ₂	1.56	1.49	1.53				

^aReference 10.^bReference 30.^cReference 39.

IV. RESULTS AND DISCUSSION

A. Cyclic C₃H

The first excited state electronic transition of c -C₃H has been assigned by Yamamoto *et al.*³ to be of $X(^2B_1) \rightarrow ^2A_1$ symmetry, and is the only experimentally reported transition so far. Using a simple model, they deduce a vertical excitation energy of 10 800 cm⁻¹ (1.339 eV). This particular excited state involves a $6a_1 \rightarrow 3b_1$ transition rather than a $3b_1 \rightarrow 7a_1$ excitation. Hence, the doubly occupied $6a_1$ orbital must be retained in the valence space. This feature also explains why the EOMCC-IP computations have been performed using the negative ion $|\Phi_{C_3H^-}\rangle$ CSF as the closed shell zeroth-order wavefunction. More specifically, the excited state of interest for the c -C₃H isomer has the CSF $|(core)^{16}6a_13b_1^2\rangle$. This particular CSF may be generated conveniently from a closed shell CSF $|(core)^{16}6a_1^23b_1^2\rangle$ by removing an electron from the occupied $6a_1^1$ orbital, thereby explaining why Stanton¹⁰ employs the EOMCC-IP method to compute the excitation energies for the c -C₃H isomer.

Table II displays the vertical excitation energies and oscillator strengths of the c -C₃H isomers as computed through third order with the H^v method. The computed lowest excitation energy for the cyclic isomer is compared with experiment¹¹ and with other high-level calculations, the CASSCF calculations of Takahashi⁸ and the equation of motion-coupled cluster singles and doubles for ionized states (EOMIP-CC) calculations of Stanton.¹⁰ The errors in the estimation of vertical excitation energy for $X(^2B_1) \rightarrow ^2A_1$ from the CASSCF, EOMIP-CC, and H^v methods (computed at the experimental geometry) are $\approx 14\%$, 4.2%, and 0.6%, respectively. However, the accuracy of the computed H^v excitation energy for the lowest $X(^2B_1) \rightarrow ^2A_1$ transition degrades when the MP2 (off by 2.8%) and H^v (off by 5.9%) optimized geometries are used in the calculations. Table I indicates that the deviation from experiment of the calculated C–H bond length $R_{C-H}^{(Opt.)} - R_{C-H}^{(Expt.)}$ is large (0.3%) compared to the deviation $R_{C-H}^{(Opt.)} - R_{C-C}^{(Expt.)}$ (0.2%) for the C–C bond length. Therefore, the slightly greater inaccuracy in the estimation of the transition energy at the optimized geometry presumably arises due to the overestimation of the C–H bond distance by the optimization procedure. Nevertheless, the estimated quantity is in accord with the experiment and state-of-the-art EOMIP-CC calculations. Interestingly, while both the CASSCF and EOMIP-CC calculations underestimate the $X(^2B_1) \rightarrow ^2A_1$ transition energy, the H^v method overesti-

mates this quantity, with the H^v and EOMIP-CC energies of comparable accuracy.

Table III summarizes the computed third-order H^v vertical ionization potentials and electron affinities for the cyclic form of the C₃H radical. To our knowledge, Table III represents the first report for the ion state energies of this radical. Unlike the vertical excitation energy, the ionization energies and the electron affinities computed at the experimental, MP2, and H^v optimized geometries are quite close to each other, indicating that the ion state vertical energies are quite insensitive to these small shifts in the geometrical parameters. The two negative electron affinities imply that the 1¹B₁ and 1³B₁ anion excited states are metastable Feshbach resonances lying in the electron detachment continuum.³⁴ A separate computation for the negative ions should probably be used to provide a more accurate description for the interesting excited anion states.

Table IV uses the two optimized and the experimental geometries to illustrate the slight variation of the computed dipole moment with the geometrical parameters. The table also compares the computed dipole moment from the third-order H^v calculations with experiment and with other correlated calculations. While the ground state dipole moments computed with the H^v method at the experimental and optimized geometries (MP2 and H^v) are reasonably close to experiment and to other correlated calculations, the dipole moment of the first excited state of A₁ symmetry is quite a bit larger than the other theoretical value, presumably because our calculations apply for the ground state geometry, while Ref. 10 uses the excited state geometry.

The vibrational frequencies obtained from the H^v method are compared with experiment³⁵ and with other theoretical calculations⁸ in Table V. The H^v method estimate for the lowest vibrational frequency of a₁ symmetry is compa-

TABLE V. Vibrational frequencies (in cm⁻¹) of the c -C₃H radical.

Symmetry	H ^v	CASSCF ^a	MP2 ^a	Experiment
a ₁	1050	1191	1206	1160 ^b
a ₁	1554	1670	1657	1832 ^b
a ₁	3712	3450	3325	3238 ^b
b ₁	1117	1047	969	508 ^c
b ₁	8303	890i	12526	

^aReference 8.^bReference 35.^cReference 26.

TABLE VI. Vertical excitation energies (in eV) and oscillator strengths (in parentheses) of the *l*-C₃H radical.

State	Third-order H^v			
	MP2 geometry	Experimental geometry	H^v geometry	Mixed geometry
$1^4\Delta$	1.970	4.329	4.064	4.370
$1^2\Sigma^+$	3.320 (0.003)	5.461 (0.009)	5.219 (0.008)	5.506
$1^2\Delta$	3.429 (0.016)	5.155 (0.021)	4.969 (0.20)	5.207
$1^2\Sigma^-$	3.978	5.957	5.697	6.000
$2^2\Delta$	5.226	5.912	5.806	5.917

able to that from the CASSCF and MP2 calculations, but the H^v overestimates the other two vibrational frequencies of the same symmetry. Both the H^v and CASSCF treatments yield unphysical results for the b_1 vibration for which CASSCF computations yield an imaginary frequency. In addition, the lowest experimental³ vibrational frequency of cyclic C₃H is 508 cm⁻¹ (a b_1 in-plane mode), and all the theoretical calculations, including the present, one fail to provide a comparable low-frequency vibration. An explanation for these behaviors emerges from an analysis of the G -matrix³⁶ for the cyclic isomer in the five-dimensional space considered (which contains two b_1 vibrations). Both computed b_1 vibrational frequencies are highly sensitive to an off-diagonal G -matrix element: changing the CCC equilibrium bond angle over a range of 2–3 degrees shifts the computed frequencies from 11 000 to 6000 cm⁻¹ for the higher frequency b_1 vibration, and a change in the CCC bond angle of 1 degree converts the lower frequency mode from \approx 1000 cm⁻¹ to an imaginary frequency. (Note that the root-mean-square zero point bending amplitude is \approx 4 degrees.) Presumably, the theoretical force constants (F -matrix) are reasonable, but the vibrational frequencies should be evaluated with G -matrix elements that are explicit functions of the angle.

The third-order H^v method compensates perturbatively for a wide range of different choices for the orbitals and orbital energies. For example, the third-order H^v vertical transition energies and other related properties for the *c*-C₃H isomer have been computed separately by using the occupied orbitals generated from a SCF sequence with the first step involving the (core)¹⁶ $6a_2^2$ (cation) configuration and those with the first step involving the (core)¹⁶ $6a_1^2 3b_1^1$ (neutral) ground state Fock operators, respectively. The occupied orbitals from the (core)¹⁶ $6a_1^2$ positive ion Fock operator clearly experience a greater attractive potential and, therefore, are more tightly bound than those generated from the neutral (core)¹⁶ $6a_1^2 3b_1^1$ Fock operator. Because the two sets

of orbitals and orbital energies differ considerably between these two extreme situations, one test of practical convergence is the degree to which the computed properties differ with the two orbital choices since infinite-order calculations should yield identical results in both cases. The use of cation and neutral occupied orbitals produces the third-order $H^v X(^2B_1) \rightarrow 1^2A_1$ transition energy as 1.347 and 1.288 eV, respectively, which is a rather minor difference. The two choices of orbitals and orbital energies yield virtually identical values for the dipole moment. Thus, both choices of orbitals are quite adequate for the cyclic isomer. However, the use of cation orbitals is more convenient and attractive computationally for the linear isomer, where this choice reduces the computational complexity during the orbital optimization.

B. Linear C₃H radical

Tables VI–IX respectively present the third-order H^v vertical excitation energies, ionization potentials, electron affinities, and dipole moments as computed at three different geometries (experimental, MP2, and H^v optimized) and the vibrational frequencies obtained from the H^v optimization process. To our knowledge, no experimental or theoretical data (except the vibrational frequencies and ground state dipole moment) are available for comparison. However, based on our success for the cyclic isomer and several other systems,^{13,14,20–23} we expect that our computed properties for the *l*-C₃H isomer should be quite accurate, and, therefore, of interest in spectroscopic studies.

It is evident from Table I that all the optimization procedures appear to fail in reproducing the exceptionally short C–H bond length of 1.017 Å determined experimentally.²⁷ The short computed C–H distance was later interpreted by Oschenfeld *et al.*³⁰ as occurring because of the Renner–Teller effect³⁷ which arises due to the very-low-lying vi-

TABLE VII. Dipole moments (in Debye) of the *l*-C₃H radical.

State	Third-order H^v			MP2 ^a	CASSCF ^a	Experiment
	MP2 geometry	Experimental geometry	H^v geometry			
$X^2\Pi$	1.83	2.46	2.41	3.31	3.42	3.1 ^b
$1^4\Delta$	0.59	1.66	1.62			
$1^2\Sigma^+$	1.38	2.35	2.35			
$1^2\Delta$	2.16	3.31	3.31			

^aReference 8.

^bReference 40.

TABLE VIII. Vertical ionization potentials and electron affinities (in eV) of the l -C₃H radicals.

State	Third-order H^v		
	MP2 geometry	Experimental geometry	H^v geometry
Ionization potential			
$1^1\Sigma$	8.701	9.327	9.208
$1^1\Pi$	12.831	15.223	14.969
Electron affinity			
$1^1\Pi$	0.298	0.221	0.305
$1^3\Pi$	0.204	0.131	0.215

bronic state involving the CCH bending mode and because the experiments only determine the projection of the C–H bond on the molecular axis. They have shown that the vibrational average for the projection of the C–H bond length on the molecular axis reduces the C–H bond length from 1.065 to 1.008 Å in much better accord with the experimentally quoted quantity. Using the same procedure, i.e., by evaluating the projection on the molecular axis of the C–H bond length as averaged over the CCH bending zero point motion, we obtain 1.019 Å for the projected C–H bond length which is very close to experiment.

Tables VI and VII demonstrate that the excitation energies and dipole moments of the l -C₃H isomer vary significantly between the different optimized geometries primarily because the single reference MP2 geometry optimization for this isomer encounters inaccuracies due to the importance of two dominant resonance structures. The MP2 geometry optimization produces a shorter C₁–C₂ bond length than experiment. The MP2 optimization yields the C₁–C₂ and C₂–C₃ bond lengths to be, respectively, of the order of the CC triple bond length in C₂H₂ (1.2033 Å) and the CC double bond length in C₂H₄ (1.3384 Å). Both the MP2 and H^v methods agree on the C–H bond length as discussed above, but the H^v geometry compares more favorably to experiment for the CC bond lengths. Since all of the theoretical methods yield the actual C–H bond length as opposed to experiment which only obtains its projection on the molecular axis, we compute the excitation energies using a “mixed experimental” geometry in which the C–C bond lengths are taken from experiment while the C–H bond length is taken from theory (the H^v optimized value). In contrast to the excitation energies evaluated for the poor MP2 geometry, the relative ordering of the excited states (except the rather nearby $1^2\Sigma^-$ and $2^2\Delta$ excited states) computed at the experimental and “mixed” geometries agrees with that calculated at the H^v geometry. The small differences arise from a slight variation in the C–C bond lengths. This analysis confirms that the

significant variation in the computed excitation energies and dipole moments between the MP2 and H^v methods as well as between the MP2 and experimental geometries arises mostly due to the poor MP2 estimate of the C–C bond lengths rather than errors in the C–H bond length.

Table VIII presents the ionization potentials and electron affinities of the linear isomer from third-order H^v calculations at the experimental and theoretically optimized geometries. The table clearly indicates that the singlet and triplet Π states of l -C₃H[−] are bound, with the $1^1\Pi$ state lower energetically than the $3^3\Pi$ electronic state as expected. It is also interesting to note that the positive and negative ion states of the l -C₃H display a dependence on geometry. While the H^v vertical ionization potentials for the H^v optimized geometry are quite close to those for the experimental geometry, the electron affinities differ substantially. A separate optimization for the positive and negative ions of the l -C₃H radical may be useful to provide a more accurate description for these interesting excited ionic species.

The harmonic vibrational frequencies obtained from the H^v geometry optimization are compared with those obtained from the CASSCF and MP2 calculation of Takahashi *et al.*⁸ and the MCSCF calculation of Kanada *et al.* in Table IX. The experimentally³⁸ estimated lowest vibration frequency for this isomer is as low as 28 cm^{−1}, which corresponds to the C–H bending mode. The present and all earlier theoretical calculations, including CASSCF, MP2, and MCSCF calculations fail to account for such a low-frequency vibrational mode. The estimated vibrational frequency for this C–H bending mode with the H^v , MP2, and CASSCF methods is 262, 245, and 325 cm^{−1}, respectively, departing considerably from experiment.

C. Conformational energy difference

Table X compares the ground state energy difference between the cyclic and linear C₃H radicals as computed

TABLE IX. Vibrational frequencies (in cm^{−1}) of the l -C₃H radical.

Isomer	Symmetry	H^v	CASSCF ^a	MP2 ^a	MCSCF ^b
	π	262	325	245	247i
	σ	1020	1095	1117	1139
	σ	1829	1925	2467	1906
	σ	3291	3613	3601	3607

^aReference 8.^bReference 27.

TABLE X. Energy difference (in KJ mol⁻¹) between the *c*-C₃H and *l*-C₃H radicals.

Third-order H^v					Approximate experiment ^c
Experimental geometry	MP2 geometry	H^v geometry	CCSD(T) ^a	MRCI ^b	
14.12	4.58	8.39	13.00	9.01 (8.62)	4.18–8.32

^aReference 30.^bReference 8.^cReference 6.

through third order with the H^v method and as obtained from experiment and from other theoretical calculations.^{7,8} Table X indicates that the third-order H^v conformational energy difference at the experimental geometry is fairly close to that obtained from the CCSD(T) method but does not fall within the experimental range. However, as noted above the experimental C–H bond length corresponds only to the projection on the molecular axis, not the actual bond length. The third-order H^v estimate for the ground state energy difference between these two isomeric forms at the respective H^v optimized geometries not only lies within the experimental range but is also quite close to the MRCI value. The computations in Table X should be modified for differences in zero point energies between the isomers. Reference 8 estimates that the zero point differences reduce the computed energy difference by 1.1 Kcal/mol, bringing the H^v calculations well within the experimental range. Further reduction in the small discrepancies between the optimized and experimental geometries may help in pinning down a more precise theoretical prediction.

V. CONCLUSION

We describe highly correlated *ab initio* computations for the ground state energy difference between the cyclic and linear isomers of propynylidyne (C₃H), as well as their harmonic vibrational frequencies, ionization potentials, electron affinities, excited state energies, dipole moments, and oscillator strengths, some of which have not been reported before. The difficulties in computing this isomer energy difference are illustrated by contrasting our computations using the theoretically optimized geometries and the experimental geometries. The third-order H^v conformational energy difference between the two C₃H isomers at the experimentally quoted geometry is in good agreement with that obtained from the CCSD(T) method but departs considerably (≈ 6 – 10 KJ/mol) from experiment, mainly because experiment for the linear geometry only provides the projection of the C–H bond on the molecular axis. On the other hand, the third-order H^v isomer energy difference computed for the H^v and MP2 optimized geometries lie at the opposite extremes of the experimental range, although inclusion of approximate zero point energy corrections place the H^v value squarely within the experimental range and the MP2 value slightly below this range. The main source of uncertainty in the energy difference probably stems from residual discrepancies between the theoretical and experimental geometries.

The H^v calculations for the ground state isomer energy difference, the cyclic C₃H lowest excitation energy, and the

dipole moments in both isomers are in good agreement with experiment and with other state-of-the-art correlated computations. These agreements once again demonstrate the high accuracy obtainable with the H^v method for complex atomic and molecular systems. We provide the first high level calculations for excitation energies and oscillator strengths to higher excited states of both isomers, as well as several lowest vertical ionization potentials and electron affinities. This new information emerges as a bonus of the H^v method which generates all states of the neutral and ions from a single computation. The computations suggest that linear anion has bound excited state. A strong sensitivity of the computed b_1 vibrational frequencies for the cyclic isomer on a G -matrix element explains the persistent difficulties in computing accurate values.

ACKNOWLEDGMENTS

Useful discussions with Professor T. Oka and Professor D. Levy are gratefully acknowledged. This research is supported, in part, by NSF Grant No. CHE-9727655.

- ¹P. Thaddeus, C. A. Gottlieb, A. Hjalmarson, L. E. B. Johansson, W. M. Irvine, P. Friberg, and R. A. Linke, *Astrophys. J. Lett.* **294**, L49 (1985).
- ²C. A. Gottlieb, J. M. Vrlitek, E. W. Gottlieb, P. Thaddeus, and A. Hjalmarson, *Astrophys. J. Lett.* **294**, L55 (1985).
- ³S. Yamamoto, S. Saito, M. Ohishi, H. Suzuki, S. Ishikawa, N. Kaifu, and A. Murakami, *Astrophys. J. Lett.* **322**, L55 (1987).
- ⁴T. J. Miller, C. M. Leung, and E. Herbst, *Astron. Astrophys.* **183**, 109 (1987).
- ⁵D. Smith, *Chem. Rev.* **92**, 1580 (1992).
- ⁶R. I. Kaiser, C. Ochsenfeld, M. Head-Gordon, Y. T. Lee, and A. G. Suits, *Science* **274**, 1508 (1996) and references therein.
- ⁷R. I. Kaiser, Y. T. Lee, and A. G. Suits, *J. Chem. Phys.* **103**, 10395 (1995).
- ⁸J. Takahashi and K. Yamashita, *J. Chem. Phys.* **104**, 6613 (1996).
- ⁹K. Akoi, K. Hashimoto, S. Ikuta, and A. Murakami, *Astrophys. J.* (in press).
- ¹⁰J. F. Stanton, *Chem. Phys. Lett.* **237**, 20 (1995).
- ¹¹S. Yamamoto and S. Saito, *J. Chem. Phys.* **101**, 5484 (1994).
- ¹²K. F. Freed, *Lecture Notes in Chemistry* (Springer, Berlin, 1989), Vol. 52, p. 1.
- ¹³H. Sun, K. F. Freed, M. Herman, and D. L. Yeager, *J. Chem. Phys.* **72**, 4158 (1980).
- ¹⁴R. K. Chaudhuri, A. Mudholkar, K. F. Freed, C. H. Martin, and H. Sun, *J. Chem. Phys.* **106**, 9252 (1997) and references therein.
- ¹⁵R. K. Chaudhuri and K. F. Freed, *J. Chem. Phys.* (to be published).
- ¹⁶S. Majumder, B. P. Das, and R. K. Chaudhuri, *Phys. Rev. A* **59**, 3432 (1999).
- ¹⁷J. E. Stevens, K. F. Freed, F. Arendt, and R. L. Graham, *J. Chem. Phys.* **101**, 4832 (1994).
- ¹⁸C. M. Taylor, R. K. Chaudhuri, and K. F. Freed (to be submitted).
- ¹⁹R. K. Chaudhuri, B. P. Das, and K. F. Freed, *J. Chem. Phys.* **108**, 2556 (1998).
- ²⁰J. P. Finley and K. F. Freed, *J. Chem. Phys.* **102**, 1306 (1995).
- ²¹R. L. Graham and K. F. Freed, *J. Chem. Phys.* **96**, 1304 (1992).

- ²²A. W. Kanzler, H. Sun, and K. F. Freed, *Int. J. Quantum Chem.* **39**, 269 (1991).
- ²³C. M. Martin and K. F. Freed, *J. Chem. Phys.* **100**, 7454 (1994).
- ²⁴J. E. Stevens, R. K. Chaudhuri, and K. F. Freed, *J. Chem. Phys.* **105**, 8754 (1996).
- ²⁵(a) J. P. Finley, R. K. Chaudhuri, and K. F. Freed, *J. Chem. Phys.* **103**, 4990 (1995); (b) J. P. Finley, R. K. Chaudhuri, and K. F. Freed, *Phys. Rev. A* **54**, 343 (1996); (c) R. K. Chaudhuri, J. P. Finley, and K. F. Freed, *J. Chem. Phys.* **106**, 4067 (1997).
- ²⁶(a) M. G. Sheppard and K. F. Freed, *J. Chem. Phys.* **75**, 4525 (1981); (b) M. G. Sheppard and K. F. Freed, *Int. J. Quantum Chem.* **15**, 21 (1981).
- ²⁷S. Kanada, S. Yamamoto, S. Saito, and Y. Osamura, *J. Chem. Phys.* **104**, 2192 (1996).
- ²⁸A. J. Sadlej, *J. Chem. Phys.* **75**, 320 (1981).
- ²⁹T. H. Dunning, *J. Chem. Phys.* **90**, 1007 (1989).
- ³⁰C. Ochsenfeld, R. I. Kaiser, Y. T. Lee, A. G. Suits, and M. Head-Gordon, *J. Chem. Phys.* **106**, 4141 (1997) and references therein.
- ³¹B. H. Brandow, *Rev. Mod. Phys.* **39**, 771 (1967).
- ³²I. Lindgren and J. Morrison, *Atomic Many-Body Theory*, 2nd ed., Springer Series on Atoms and Plasmas (Springer, New York, 1986).
- ³³R. K. Chaudhuri, J. E. Stevens, and K. F. Freed, *J. Chem. Phys.* **108**, 9685 (1998).
- ³⁴H. Sun and K. F. Freed, *J. Chem. Phys.* **76**, 5051 (1982).
- ³⁵M. E. Jacox, in *Vibrational and Electronic Energy Levels of Polyatomic Transient Molecules*, edited by J. W. Gallagher (American Chemical Society and American Institute of Physics for NIST, Gaithersburg, MD, 1993), p. 156.
- ³⁶E. Bright Wilson, Jr., J. C. Decius, and P. C. Cross, *Molecular Vibrations (The Theory of Infrared and Raman Vibrational Spectra)* (Dover, New York, 1980).
- ³⁷G. Herzberg, *Molecular Spectra and Molecular Structure* (Krieger, Malabar, 1991), Vol. III.
- ³⁸S. Yamamoto, S. Saito, H. Suzuki, S. Deguchi, N. Kaifu, S. Ishikawa, and M. Ohishi, *Astrophys. J.* **348**, 363 (1990).
- ³⁹J. M. Vrtilik, C. A. Gottlieb, T. C. Killian, and P. Thaddeus, *Astrophys. J. Lett.* **364**, L53 (1989).
- ⁴⁰F. J. Lovas, R. D. Suenram, T. Ogata, and S. Yamamoto, *Astrophys. J.* **399**, 325 (1992).